Explor. Mining Geol., Vol. 9, Nos. 3 and 4, pp. 171-188, 2000

0964-1823/00 $17.00 + .00

Geologic Setting, Geochemistry of Alteration, and U-Pb Age of Hydrothermal Zircon from the Silurian Stog'er Tight Gold Prospect, Newfoundland Appalachians, Canada

J. RAMEZANI*, G.R. DUNNING and M.R. WILSON
Department of Earth Sciences, Memorial University
St. John's, Newfoundland, Canada, A1B 3X5

Received September 5, 2000; accepted May 9, 2001.

Abstract — The early Paleozoic accretionary tectonic regime that was established along the Laurentian margin of the Newfoundland Appalachians provided a favorable setting for shear-hosted gold mineralization along a major terrane suture, the Baie Verte-Brompton Line. The Stog'er Tight prospect is one of several mesothermal-style gold occurrences hosted by shear zones within accreted ophiolites and oceanic arc terranes on the Baie Verte Peninsula. It is an epigenetic, stratabound deposit that is confined to shallow-level gabbro sills within the volcanic cover sequence of the allochthonous Point Rousse ophiolite complex. Gold mineralization at Stog'er Tight is associated with hydrothermal mineral assemblages represented by chlorite-calcite, sericite-ankerite, red albite-pyrite (±Au) and chlorite-magnetite alteration zones. Gold occurs with pyrite within the intensely altered gabbro, along the margins of syn- to late-shear, quartz-rich, replacement veins.

The Stog'er Tight gabbro served as a rigid body conducive to shear deformation and fluid penetration, whereas, its high Fe-Ti oxide content induced fluid oxidation and gold-pyrite precipitation. Hydrothermal alteration involved progressive CO_2, S, Na, and LILE metasomatism, along with significant enrichments in the REE, HFSE, and Th in the high-grade ore zone. Temperatures of vein formation and alteration are constrained by oxygen isotope thermometry to be between 250°C and 480°C. Isotopic compositions of vein quartz from the Stog'er Tight prospect are uniform ($\delta^{18}O$ = +12.5 ± 1‰) and fall within the range cited for many shear-hosted, auriferous quartz veins.

A U-Pb zircon igneous age of 483 +3/-2 Ma for the Stog'er Tight gabbro is consistent with its stratigraphic correlation with other Ordovician ophiolitic and volcanic arc/back-arc assemblages in Newfoundland. The U-Pb age of a rare variety of hydrothermal zircon recovered from the high-grade ore zone directly constrains the timing of gold mineralization to 420 ±5 Ma, in accord with a major orogenic episode of Silurian age that produced many of the magmatic and metamorphic rock suites in north-central Newfoundland. Our results are consistent with a post-peak metamorphic, late-magmatic model for gold mineralization that occurred during the waning stages of Silurian orogenesis, driven by emplacement of I-type granitoid intrusions into the crust.

Introduction

Mesothermal lode gold deposits are not uniformly distributed through geologic time. Most occur in the Late Archean, with a smaller number in the Late Proterozoic and Mesozoic. With few exceptions, lode gold associated with greenstone belts and mixed ultramafic-volcanic assemblages are uncommon in the Paleozoic (Hutchinson, 1987; Keays and Skinner, 1989). Given that accretionary tectonic processes have been viewed as a crucial element in the genesis of gold deposits of all ages (e.g., Barley et al., 1989; Hodgson et al., 1990; Kerrich and Wyman, 1990), the general absence of significant economic deposits of this type in the Paleozoic accreted oceanic terranes of the Appalachian Orogen remains unexplained. There are, however, many examples of mesothermal gold occurrences documented from the Meguma terrane of Nova Scotia and the Dunnage Zone of Newfoundland (e.g., Tuach et al., 1988; Dubé, 1990; Kontak et al., 1990). These occurrences bear important clues to the spatial and temporal relationships of gold mineralization to Paleozoic accretionary processes.

In western Newfoundland, Proterozoic (Grenville) basement and its overlying shelf-facies strata of the North American (Laurentian) continental platform are over-ridden from the east by allochthonous ophiolitic and oceanic volcanic/epiclastic rocks (Williams and Stevens, 1974). In the area of the Baie Verte Peninsula, the accreted oceanic terranes are separated from metasedimentary rocks of the Laurentian margin by the Baie Verte-Brompton Line (Fig. 1), a narrow structural zone characterized by discontinuous ophiolite slivers (Williams and St-Julien, 1982). Both sides of the terrane boundary are intruded by granitic plutons and display evidence of widespread rock deformation and fluid-

*Present Address: Department of Earth, Atmospheric and Planetary Sciences, Massachusetts Institute of Technology, Bldg. 54-1020, Cambridge, MA 02139, U.S.A.

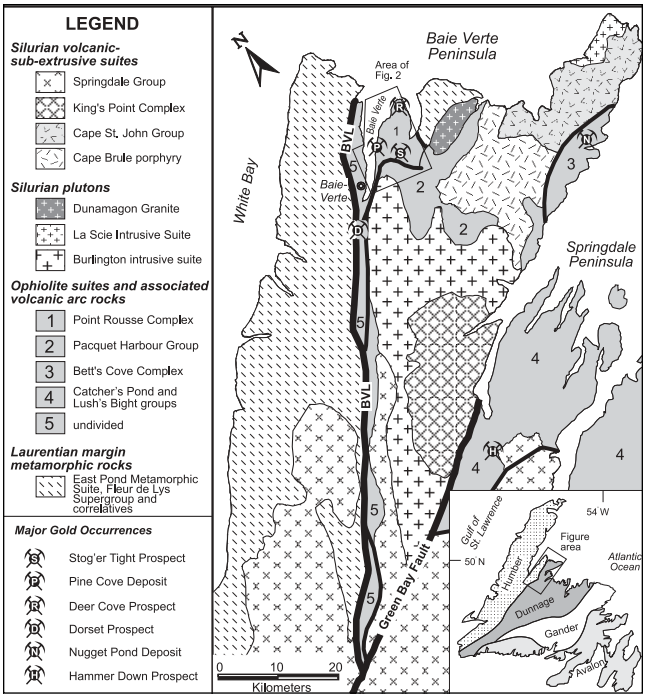

Fig. 1. Regional geologic map of the Baie Verte Peninsula showing the major lithostratigraphic units and igneous intrusions on both sides of the Baie Verte Line (BVL), and the locations of major gold occurrences. Map is compiled after Hibbard (1983), Mercer et al. (1985), Kean and Evans (1987), and Ritcey et al. (1995) with modifications. Inset: major lithotectonic zones of Newfoundland (Williams, 1979).

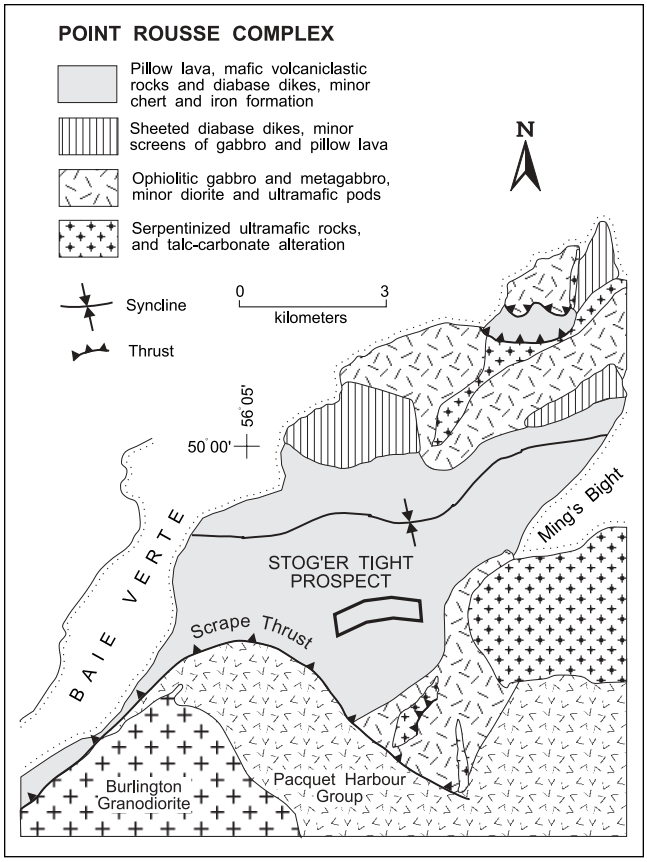

Fig. 2. Geologic map of the Point Rousse Complex (after Hibbard, 1983), and the location of the Stog'er Tight gold prospect.

rock interaction. These include regional- to local-scale faults and shear zones, vein systems, and hydrothermal alteration in fracture networks. The largest hydrothermal systems are associated with several mesothermal gold occurrences (e.g., Deer Cove, Pine Cove, Stog'er Tight and Nugget Pond; Fig. 1). The Nugget Pond deposit (Richmont Mines Inc.) is the only current gold producer on the Baie Verte Peninsula and currently accommodates the only active gold mill in Newfoundland.

Well-constrained geologic-age relationships in the northern Baie Verte Peninsula along with the remarkable alteration features of the Stog'er Tight prospect provide a unique opportunity to investigate gold-mineralizing processes in north-central Newfoundland. This study describes the geologic setting and alteration features of the Stog'er Tight gold prospect and uses combined petrographic, trace element and oxygen isotope analyses to constrain the nature of the ore-forming processes. We report new U-Pb ages for the host gabbro, and for a rare variety of hydrothermal zircon recovered from the mineralized zones of the Stog'er Tight prospect. The new data are interpreted in the context of recent geochronologic work that has identified distinct Ordovician and Silurian orogenic events in Newfoundland (Dunning et al., 1990; Cawood et al., 1994) in connection to the accretion of oceanic volcanic terranes onto the ancient margin of the North American continent.

Regional and Local Geology

Introduction

In Newfoundland, Cambro-Ordovician ophiolite complexes, oceanic volcanic arc sequences and marine epiclastic rocks collectively comprise the Dunnage Zone (Notre Dame Subzone) which was accreted to the basement and shelf rocks of the ancient Laurentian margin (Fig. 1, inset). The present-day boundary between the continental and oceanic terranes is marked by a major structural discontinuity called the Baie Verte-Brompton Line, which can be traced along the Appalachian Orogen for hundreds of kilometers (Williams and St-Julien, 1982). Its northernmost segment in Newfoundland (Fig. 1) is known simply as the Baie Verte Line (Hibbard, 1983).

On the Baie Verte Peninsula, the Baie Verte Line is a complex suture zone marked by highly deformed ophiolitic rocks and melanges. It separates poly-deformed schists, gneisses, and migmatites of the Fleur de Lys Supergroup and East Pond Metamorphic Suite, interpreted to constitute part of the Laurentian continental margin, from four accreted Ordovician ophiolite suites and their volcano-sedimentary cover sequences (Hibbard, 1983). The ophiolite suites include the Advocate, Betts Cove and Point Rousse complexes, and the Pacquet Harbour Group (Fig. 1). By

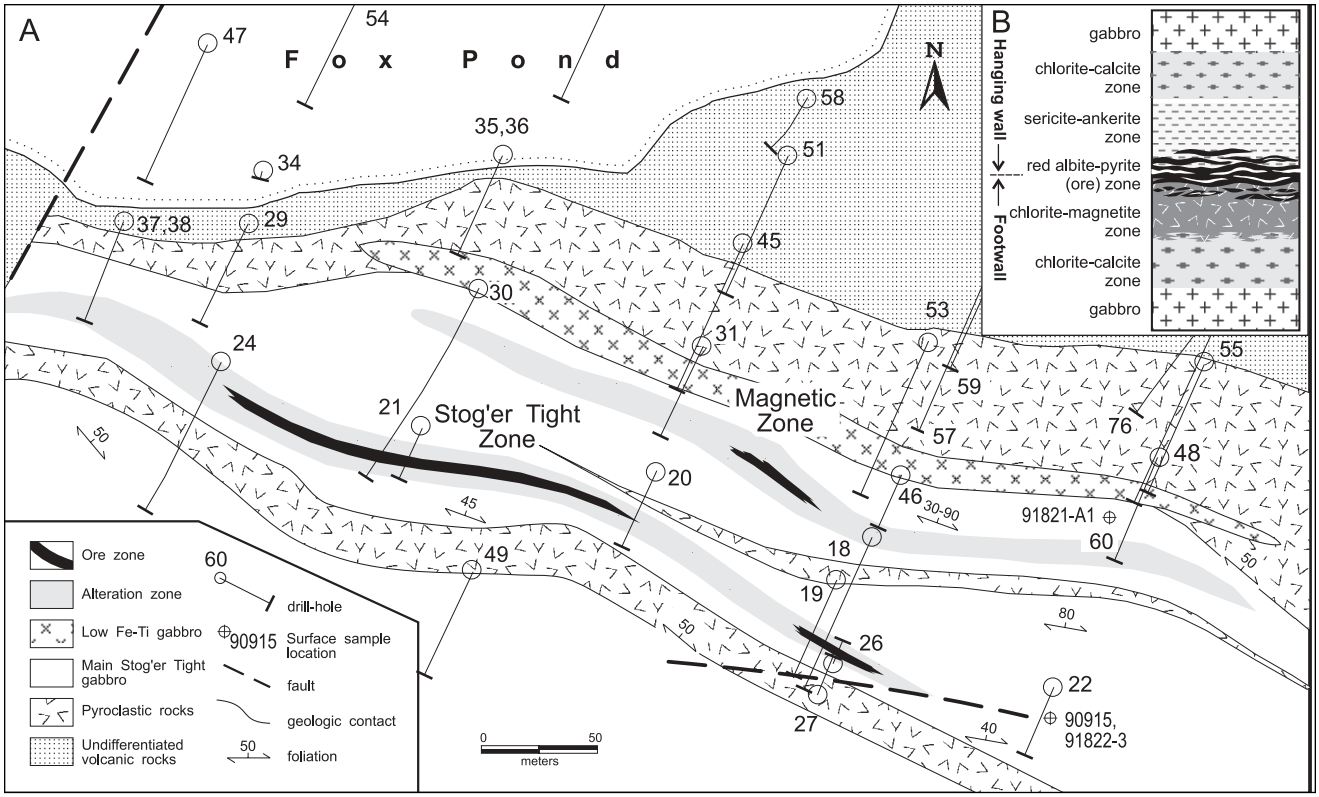

Fig. 3. (A) Geologic map of the eastern section of the Stog'er Tight gold prospect incorporating the 'Stog'er Tight' and 'Magnetic' ore zones. Compiled after the Noranda Exploration Co. unpublished map with modifications. (B) Schematic cross-section showing the alteration zonation and mineralization.

analogy to other areas in western Newfoundland, allochthon emplacement is attributed to the Taconian (Ordovician) tectonic event. The continental and oceanic terranes on both sides of the Baie Verte Line are cut by mafic to felsic intrusions of documented Silurian age (Cawood and Dunning, 1993; Cawood et al., 1994).

Point Rousse Complex

The Point Rousse Complex is a structurally disrupted, but complete, ophiolite that is exposed in an east-west trending synclinorium near the northern coast of the Baie Verte Peninsula (Fig. 2). It contains serpentinized ultramafic rocks, gabbro, sheeted dikes, and pillow lavas, and has a conformable cover sequence of mafic volcanic and pyroclastic rocks (Norman and Strong, 1975; Kidd et al., 1978). The ophiolite is interpreted to structurally overlie metasedimentary rocks of the Fleur de Lys Supergroup. It is separated from the Pacquet Harbour Group to the south by the Scrape Thrust, and from metasedimentary rocks of the Mings Bight Group (also part of the Laurentian margin) to the east by a high angle fault zone (Hibbard, 1983). According to Kirkwood and Dubé (1992), the main phase of the deformation (D_I) in the southern portion of the Point Rousse Complex (including the Stog'er Tight prospect) generated east-west trending folds and axial planar faults, together with south-verging thrust displacement sub-parallel to the Scrape Thrust (Fig. 2). Gold mineralization in the Stog'er Tight prospect is confined to the D_I shear zones.

Stog'er Tight Gabbro

The volcanic cover sequence of the Point Rousse ophiolite is intruded by several late-stage mafic sills that host the Stog'er Tight gold occurrences (Fig. 3). The gabbro sills range in thickness from 11 m to 70 m and have evident chilled margins. The gabbros typically consist of plagioclase (45% to 60%), amphibole (45% to 30%) and ilmenomagnetite (7% to 20%), with subordinate amounts (≤5%) of epidote, chlorite, quartz, titanite, apatite and zircon. Plagioclase has an albitic composition (An<10), whereas, the amphibole shows morphologic evidence indicating replacement of primary hornblende by low-Al actinolite. Ilmenomagnetite is variably altered to an amorphous assemblage of hydrous titanium silicates and oxides commonly referred to as *leucoxene*. Though the sills are collectively termed "gabbro" (e.g., Kirkwood and Dubé, 1992), the main Stog'er Tight meta-gabbro body that hosts mineralization can be distinguished lithologically from an adjacent, barren, low Fe-Ti meta-gabbro (or diorite) sill located to the north (Fig. 3A), primarily based on ilmenomagnetite content. The dominant albite-actinolite-epidote mineral assemblage of the Stog'er

Tight meta-gabbro is characteristic of greenschist metamorphic facies, in accord with the regional low-grade metamorphism of the Point Rousse Complex. The prefix 'meta' is nevertheless omitted and the term gabbro is used throughout this text to refer to the metamorphosed but hydrothermally unaltered host rock at Stog'er Tight.

Hydrothermal Alteration and Gold Mineralization

Alteration Mineralogy and Zonation

The Stog'er Tight gold prospect (STGP) comprises four distinct mineralized zones (Huard, 1990), of which only the principal Stog'er Tight Zone and Magnetic Zone (Fig. 3A) were part of this study. Mineralization occurs in and adjacent to shear zones in the main gabbro body and is surrounded by a hydrothermal alteration envelope that overprints the greenschist facies mineral assemblage of the gabbro. The typical width of the alteration envelope in drill-core is about 15 m, though haloes as wide as 40 m have been observed. The alteration envelope is subdivided, based on characteristic mineral assemblages, into four distinct zones, with a somewhat asymmetric zonation in the footwall and hangingwall (Fig. 3B). In order of increasing intensity of alteration, these are: (I) chlorite-calcite zone, (II) sericite-ankerite zone, (III) red albite-pyrite (± gold) zone, and (IV) chlorite-magnetite zone (Ramezani, 1993).

The weakest intensity of alteration, furthest from mineralization, is characterized by the replacement of metamorphic actinolite by chlorite, and partial replacement of epidote by calcite. Calcite may constitute up to 10% of the rock volume. The interval between the chlorite-calcite zone and the mineralization is characterized by a distinct change in rock color from grayish-green to a pale yellow, corresponding to the introduction of sericite, and up to 50% modal ankerite (ferroan dolomite). In the sericite-ankerite zone, epidote is absent and chlorite is sparse, but gray plagioclase is still present as relict grains and as part of a fine-grained, mylonitic quartz-albite matrix.

The sericite-ankerite zone grades into a discontinuous zone of strong mineral replacement involving abundant red-colored albite, pyrite and, locally, gold, which represents the highest intensity of hydrothermal alteration. Individual, mineralized red albite-pyrite lenses up to 40 cm in thickness occur in the central parts of this zone. The presence of large (7 mm in diameter) red albite porphyroblasts comprising up to 80% of the altered rock, and the absence of a fine-grained mylonitic matrix suggest strong, syn- to late-deformational, recrystallization and annealing. Near-complete replacement of leucoxene by hydrothermal rutile occurs within the red albite-pyrite (± gold) zone.

The immediate footwall of the mineralized zone (Fig. 3B) typically occurs as a dark green, chlorite-dominated alteration interval with a distinct cataclastic (brittle or ductile-brittle) style of deformation. This zone is dominated by albite porphyroclasts in a matrix of chlorite, carbonate (both ankerite and calcite), magnetite and fine-grained quartz. The magnetite is homogeneous and Ti-free, and thus distinct from the primary ilmenomagnetite in the host gabbro. The chlorite-magnetite zone contains the largest grains of leucoxene (relict ilmenomagnetite), suggesting that this zone originally may have been part of the coarse-grained center of the sill. Structural and textural evidence, such as chlorite-filled fractures across the strained albite porphyroclasts, indicate that the chlorite-magnetite alteration partially overprinted the red albite-pyrite alteration and thus was developed late in the alteration/ mineralization history of the STGP.

The association with shear deformation, alteration mineralogy, presence of Fe-carbonate in hydrothermal veins (see below) and altered wall rock, and the absence of argillic alteration in the STGP are first-order characteristics suggestive of a mesothermal style of gold mineralization.

Gold mineralization

Quartz veins are abundant in the area of the STGP (Kirkwood and Dubé, 1992) as in most shear-hosted, mesothermal gold deposits (Kerrich, 1989a). In the Stog'er Tight Zone and the Magnetic Zone, two major types of veins occur: dilational, barren, quartz veins (fracture fills), and shear-parallel, quartz-albite-ankerite veins, the latter being restricted to the red albite-pyrite alteration zone. The shear-parallel veins (Fig. 3B) are normally less than 10 cm wide, may contain minor amounts of sericite, chlorite, and tourmaline, and have gradational boundaries with the strongly altered (albitized) host rock. The veins exhibit textural evidence of syn- to late-deformational mineral precipitation, such as undulose extinction in quartz and bent twin planes in albite porphyroblasts.

Gold is largely restricted to the altered wall rock adjacent to shear-parallel veins and also occurs in highly altered gabbro not directly associated with any veins. Gold occurs as inclusions and seams up to 100 μm in diameter inside aggregates of pyrite. The gold-bearing pyrite occurs in close textural association with relict ilmenomagnetite (leucoxene) that is replaced by hydrothermal rutile.

The mineralized wall rock is dominated by red albite, contains several percent coarse pyrite, with minor amounts of sericite, ankerite, chlorite, and apatite. Initial exploration diamond drilling in excess of 8000 m in 80 holes was carried out on the greater Stog'er Tight property by Noranda Exploration Co. Ltd. during the late 1980s and early 1990s (the property is at present owned by Ming Minerals Inc.). The highest measured ore grade in drill-core reached 68.0 g/t Au over a 0.6 m interval (Huard, 1990). Electron microprobe (EDS) analyses of gold grains reveal less than 10% Ag content, and no detectable As, Sb, Bi, or Te.

Petrographic examination, aided by electron microprobe analysis, has identified inclusions of zircon and a vari-

ety of phosphate minerals, including monazite and xenotime (yttrium phosphate), in the red albite-pyrite and chlorite-magnetite alteration zones. These inclusions locally reach up to 100 μm in diameter. The zircon has an atypical red color, generally has anhedral to subhedral morphologies, and is evidently of hydrothermal origin. It is distinct from the clear, euhedral, magmatic or metamorphic zircon, including those found in the unaltered gabbro.

Geochemical and Isotopic Analyses

Major and Trace Element Compositions

A total of 36 specimens from the major rock types and their hydrothermally altered equivalents were analyzed for their major and trace element compositions (representative analyses are listed in Appendices 1 and 2). Major oxide concentrations were measured by ICP-OES at the Newfoundland Department of Mines and Energy. Trace elements were analyzed by XRF on pressed powder pellets, and by ICP-MS using the sodium peroxide sinter technique at Memorial University. Details of the sinter technique, ICP-MS measurement statistics and laboratory standard runs are reported in Longerich et al. (1990).

Unaltered samples from the main Stog'er Tight gabbro body and the low Fe-Ti gabbro sill, as well as the host volcanic rocks in the area, range in chemical composition from monzodiorite and diorite to gabbro. Each group has distinct trace element characteristics (Fig. 4A). The volcanic rocks, part of the cover sequence of the Point Rousse ophiolite, range in composition from slightly LREE-depleted, tholeiitic basalts to LREE-enriched, sub-alkaline andesites. On the mantle-normalized trace element diagrams, all of the volcanic samples exhibit a prominent negative Nb (also Ta) anomaly coupled with a positive Th anomaly relative to the REE of similar compatibility (e.g., La and Ce). This chemical feature is characteristic of volcanic rocks in magmatic arc settings (e.g., Pearce and Cann, 1973; Wood et al., 1979). In contrast, the main gabbro samples from both drill-core and outcrop are characterized by a consistent, moderate LREE enrichment and negative Th anomaly (Fig. 4A), similar to those of enriched (E-type) MORB basalts (Sun and McDonough, 1989). The low Fe-Ti gabbro samples have a relatively flat REE pattern with slight negative Nb and positive Th anomalies interpreted to be transitional between island-arc and E-type MORB compositions. The variations in chemistry of the volcanic and gabbroic rocks are interpreted to reflect a transition from primitive to mature island-arc volcanism, followed by MORB-dominated magmatism (sill emplacement) associated with arc-rifting and back-arc basin formation. A similar compositional trend has been reported for the oceanic volcanic rocks of the Snooks Arm Group overlying the Betts Cove ophiolite complex in the eastern Baie Verte Peninsula (Jenner and Fryer, 1980).

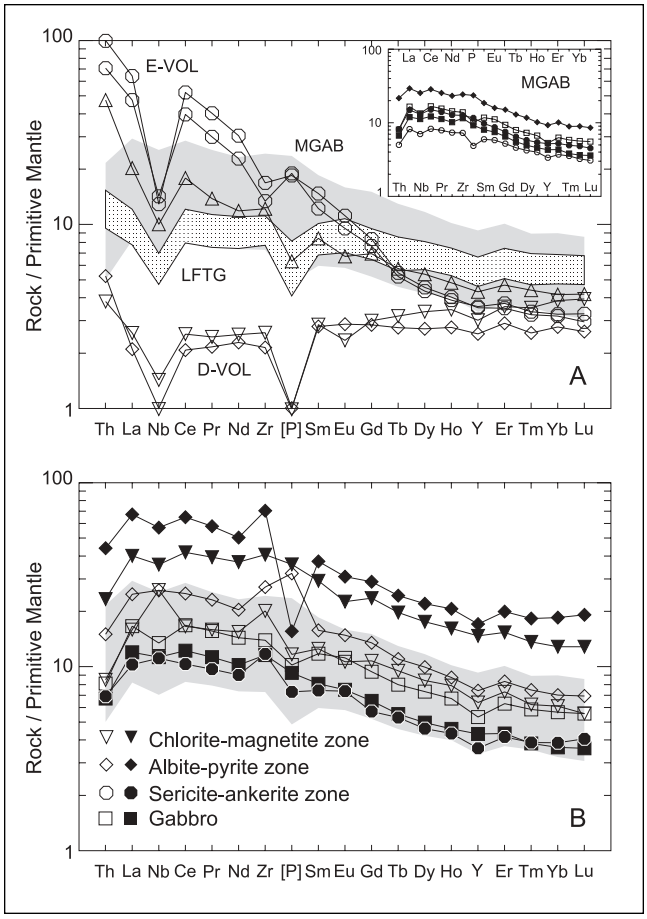

Fig. 4.(A) Mantle-normalized extended REE plot for the major rock units of the Stog'er Tight prospect. D-VOL = depleted volcanic, E-VOL = enriched volcanic, LFTG = low Fe-Ti gabbro, MGAB = main gabbro, [P] = P_2O_5. Inset shows trace element profile of the main gabbro. (B) Mantle-normalized trace element plot for alteration assemblages from drill holes 24 (solid symbols) and 53 (open symbols). Shaded area delineates trace element profile of the main gabbro. Data are from Appendices 1 and 2 (measured compositions). Primitive mantle normalizing values from McDonough and Sun (1995).

The suite of altered gabbro samples from the STGP was collected from three cross-sections through the alteration/mineralization zone represented by drill holes BN88-24, BN88-53, and BN88-55 (Fig. 3A). Representative analyses are reported in Appendix 2. Vein components, and quartz in particular, were avoided in sampling the altered rocks for geochemistry. In general, hydrothermal alteration is associated with prominent enrichments in S and the large ion lithophile elements (LILE), such as K, Rb, and Ba, along with strong depletions in the siderophile elements, Cr and Ni, relative to the precursor (unaltered gabbro) concentrations. The LILE and S enrichments are particularly strong in the sericite-ankerite and red albite-pyrite alteration zones. A distinct chemical feature of alteration at Stog'er Tight is an elevation in the REE, HFSE (Ti, Zr, Hf, Nb, and Ta) and Th concentrations in proximity to mineralization (Fig. 4B). The red albite-pyrite alteration zone bears the

Table 1. U-Pb data

Fractions		Concentrations*				Atomic Ratios**								Ages (Ma)	
No.	Properties	Weight (mg)	U (ppm)	$Pb_{rad.}$ (ppm)	Pb_{common} (pg)	$^{206}Pb/^{204}Pb$	$^{208}Pb/^{206}Pb$	$^{206}Pb/^{238}U$	±	$^{207}Pb/^{235}U$	±	$^{207}Pb/^{206}Pb$	±	$^{206}Pb/^{238}U$	$^{207}Pb/^{206}Pb$
Stog'er Tight Gabbro (sample 90915)															
G-1	20 euhedral zircon prisms, abraded	0.012	568	64.9	29	1146	.6610	.07720	52	.6041	44	.05675	18	479	482
G-2	Best clear zircon prisms, abraded	0.042	629	68.0	20	6283	.6006	.07563	46	.5921	33	.05678	20	470	483
G-3	Angular zircon fragments	0.058	961	102.6	85	3083	.6106	.07429	28	.5816	24	.05678	8	462	483
G-4	35 cracked zircon prisms	0.015	767	82.3	21	2471	.6600	.07246	78	.5669	60	.05674	14	451	482
Alteration Zone (sample BN60-37)															
H-1	5 red zircon, abraded	0.005	332	30.6	73	114	.5331	.06728	74	.5115	107	.05513	94	420	418
H-2	3 red zircon, abraded	0.003	226	20.0	12	257	.5242	.06505	38	.4944	68	.05512	66	406	417

Notes

*Uncertainty in weight is ±0.006 mg (2σ).

**Corrected for fractionation, spike, laboratory blanks of 10 to 15 pg for Pb and 1 pg for U, and initial common lead calculated from the model of Stacey and Kramers (1975). Absolute uncertainties on the isotopic ratios are reported as 2σ after the ratios and refer to the final digits; rad. = radiogenic.

strongest enrichment of these trace elements relative to the host gabbro, consistent with the occurrence of U- and REE-bearing accessory minerals, such as hydrothermal zircon, monazite, and apatite, in this zone.

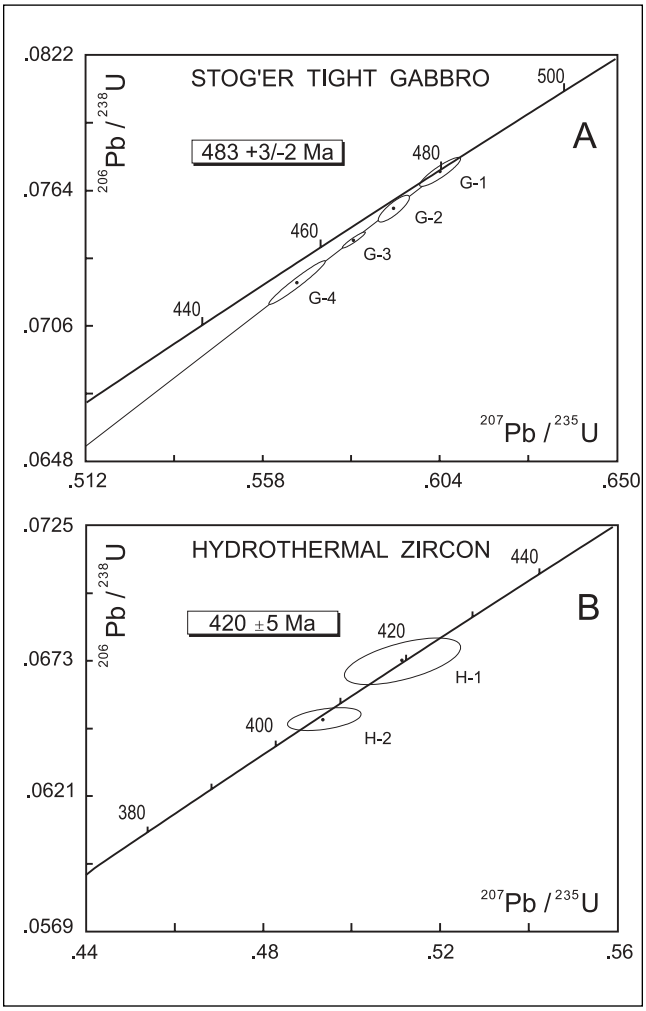

Fig. 5. U-Pb concordia diagrams for igneous zircon from the Stog'er Tight gabbro, (A), and hydrothermal zircon from the high-grade ore zone (B). Data are from Table 1.

U-Pb Zircon Geochronology

Igneous zircon was separated from a 25 kg sample of unaltered, coarse-grained gabbro for age determination. Selected zircon grains were clear, euhedral, simple prisms with pyramidal tips, which were hand-picked and grouped into four multi-grain fractions based on grain quality. Hydrothermal zircon grains from the mineralized red albite-pyrite alteration zone were small (20 μm to 80 μm), red-colored and largely suhedral to anhedral. A few grains showed twinned prisms with a morphology clearly distinct from that of the igneous zircon. The latter grains were hand-picked and individually analyzed by electron microprobe (EDS) to confirm their identity before selection for U-Pb analysis.

Sample preparation and analytical procedures including air-abrasion technique, zircon dissolution, and ion-exchange chemistry are essentially similar to those of Krogh (1973, 1982a, 1982b). Isotopic measurements were made at Memorial University on a Finnigan MAT 262 thermal-ionization mass spectrometer equipped with a secondary electron multiplier, in an ion pulse-counting mode. The measured isotopic ratios, U and Pb concentrations, calculated atomic ratios and the corresponding ages are given in Table 1. Age uncertainties are calculated using an unpublished error propagation routine modified after that devised by L. Heaman and are plotted as ellipses on conventional U-Pb concordia diagrams (Fig. 5). Concordia intercept ages and uncertainties are calculated using the linear regression method of Davis (1982). Further details of the procedure are reported in Dubé et al. (1996).

Zircon fractions from the gabbro yielded one concordant (G-1), and three variably discordant (G-2 through G-4) analyses consistent with their grain quality (Fig. 5A). All four analyses regress, with an 88% probability of fit, to a discordia line with a calculated upper intercept age of 483 +3/-2 Ma. This age is interpreted as the crystallization age of the Stog'er Tight Gabbro.

Two multi-grain fractions of red hydrothermal zircon produced analyses that are concordant within uncertainties (H-1 and H-2), but do not overlap (Fig. 5B). The uncertain-

ties associated with these analyses are influenced by small fraction sizes (5 μg and 3 μg, respectively), which increases the relative proportion of common Pb to radiogenic Pb in the analysis. The comparatively younger ages measured from H-2 are probably due to small amounts of lead loss after crystallization. The $^{206}Pb/^{238}U$ age of H-1 (420 ±5 Ma) is least affected by the common Pb corrections and is consistent with the $^{207}Pb/^{206}$ Pb ages of both fractions (ca. 418 Ma and 417 Ma), as well. The 420 ±5 Ma age is therefore interpreted as the crystallization age of the hydrothermal zircon, in association with the red albite-pyrite (± Au) alteration.

Stable Isotope Geochemistry

Mineral separates of quartz, albite, chlorite, sericite, and ankerite from veins and altered wall rocks were prepared by conventional methods (heavy liquids, magnetic susceptibility and hand-picking) and were checked for purity by XRD prior to isotopic analysis. Mineral fractions were reacted overnight with BrF_5 at 600°C (Clayton and Mayeda, 1963) to produce CO_2 for oxygen isotope analysis. CO_2 was liberated from carbonate (ankerite) by reaction with anhydrous phosphoric acid at 25°C (McCrea, 1950) for

Table 2. Oxygen and carbon isotope data for whole rocks and hydrothermal minerals of the Stog'er Tight Prospect, calculated equilibration temperatures and the oxygen isotope composition of the hydrothermal fluids

Sample No.*	$\delta^{18}O$ (‰)	$\delta^{13}C$ (‰)	Equilib T (°C)**	$\delta^{18}O_{water}$ (‰)	Comments
BN24-09	8.9 (w/r)				Red alb-pyr alteration zone
BN29-A31	13.2 (qtz)		349[1]	7.9[2]	Altered gabbro in red alb-pyr zone
	10.9 (alb)				
91822-A	12.1 (qtz)				Shear-parallel vein in mineralized gabbro
91814-C2	12.6 (qtz)				Shear-parallel vein in mineralized gabbro
BN60-42	12.5 (qtz)		316[1]	6.2[2]	Shear-parallel, mineralized vein in red alb-pyr zone
	10.1 (alb-1)		246[2,4]		(alb-1 is from host rock and alb-2 is from vein)
	10.0 (alb-2)				
	4.5 (chl)				
BN60-34	11.5 (qtz)		480[1]	8.9[2]	Shear-parallel vein in red alb-pyr zone
	9.9 (alb)		438[2,3]		
	9.0 (ser)				
	11.0(ank)	-6.9			
91814-A4	12.6 (qtz)				Dilational vein in strongly altered gabbro
BN29-22A	12.4 (qtz)		316[1]	6.1[2]	Dilational vein in red alb-pyr zone
	9.9 (alb)		282[2,3]		
	8.7 (ser)				
BN45-A30	11.9 (qtz)		345[1]	6.5[2]	Dilational vein in red alb-pyr zone
	9.6 (alb)		292[2,4]		
	4.9 (chl)				
BN60-20	11.6 (qtz)				Dilational vein in ank-ser zone
BN24-17	8.8 (w/r)				Chl-mgt alteration zone
BN24-14	4.8 (chl)				Altered gabbro in chl-mgt zone
BN29-B5	4.4 (chl)				Altered gabbro in chl-mgt zone
BN60-A8	4.8 (chl)				Altered gabbro in chl-mgt zone
BN60-48	12.5 (qtz)		377[1]	7.9[2]	Dilational vein in chl-mgt zone
	10.4 (alb)				
	11.2 (ank)	-5.6			
91814-A6	12.1 (qtz)				Dilational vein in moderately altered gabbro
91814-A8	12.5 (qtz)				Dilational vein in strongly foliated gabbro
91814-D1	12.5 (qtz)				Dilational vein in strongly foliated gabbro
91814-D2	12.7 (qtz)				Stockwork quartz in brecciated gabbro
91822-B	12.2 (qtz)				Shear-parallel vein in strongly foliated gabbro
BN60-19	12.5 (qtz)		360[1]	7.5[2]	Vein at the volcanic rocks — gabbro contact (no alteration)
	10.3 (alb)				
BN60-09	13.5 (qtz)		335[2,4]	7.7[2]	Dilational vein in volcanic rock (no alteration)
	7.3 (chl)				
BN60-101	12.0 (qtz)		400[2,3]	7.9[2]	Dilational vein in volcanic rock (no alteration)
	9.3 (ser)				
	11.4 (ank)	-6.1			
BN60-A1	13.0 (qtz)				Vein in volcaniclastic rocks (no alteration)
BN24-01	8.4 (w/r)				Main Stog'er Tight gabbro
BN55-B5	8.6 (w/r)				Low Fe-Ti gabbro
BN55-B9	8.9 (w/r)				Low Fe-Ti gabbro
BN54-B5	8.3 (w/r)				Volcanic rock (calc-alkalic)
BN54-R	8.6 (w/r)				Volcanic rock (tholeiitic)

Notes

* Sample numbers starting with BN are from drill-core, the following two digits correspond to drill-hole number (see Fig. 3 for locations). All others are trench or outcrop (surface) samples.

** Calculated equilibrium temperatures and oxygen isotope compositions of aqueous fluids are based on the following oxygen isotope fractionation factors: [1]quartz-albite (Clayton and Kieffer, 1991); [2]quartz-water (Matsuhisa et al., 1979); [3]muscovite-water (O'Neil and Taylor, 1969); and [4]chlorite-water (Wenner and Taylor, 1971).

Abbreviations: alb = albite, ank = ankerite, chl = chlorite, mgt = magnetite, ser = sericite, pyr = pyrite, qtz = quartz, w/r = whole rock.

72 hours. The isotopic compositions of CO_2 gas were measured on a Finnigan MAT 252 mass spectrometer at Memorial University. The isotopic results are reported in the standard δ notation in per mil (‰) relative to SMOW for oxygen, and PDB for carbon (Table 2).

The $\delta^{18}O$ values of eight whole rock samples of unaltered and altered gabbro and volcanic rocks define a narrow range from +8.3 to +8.9. The $\delta^{18}O$ values of quartz in 19 shear-parallel and dilational veins range from +11.5 to +13.5. Albite from veins and altered wall rock has $\delta^{18}O$ values from +9.6 to +10.9, sericite from +8.7 to +9.3, and chlorite from +4.1 to +7.3. Quartz-albite oxygen isotope thermometry yields equilibration temperatures from 320°C to 480°C, quartz-sericite from 280°C to 440°C, and quartz-chlorite from 250°C to 340°C. Three samples of ankerite from both shear-parallel and dilational veins yielded $\delta^{13}C$ values of -5.6, -6.1, and -6.9 along with $\delta^{18}O$ values of +11.2, +11.4, and +11.0, respectively.

The hydrothermal minerals from the STGP yield oxygen isotope equilibration temperatures of 250°C to 480°C that overlap with, but fall on the high end of, the temperature range reported for mesothermal gold deposits (generally 250°C to 400°C; McCuaig and Kerrich, 1998). The average equilibration temperatures for coexisting quartz-albite pairs in the STGP (360°C) are largely comparable to those for quartz-sericite (370°C), reflecting isotopic equilibrium, but are systematically higher than those for quartz-chlorite (290°C). This is consistent with petrographic evidence that hydrothermal chlorite and sericite do not coexist in the same alteration assemblage. The fluids in isotopic equilibrium with the different hydrothermal mineral assemblages are calculated to have $\delta^{18}O$ values from +6.1 to +8.9 (Table 2), which overlap with those cited for primary magmatic fluids (e.g., Sheppard et al., 1969), but these values do not uniquely discriminate between magmatic and metamorphic sources for the ore-forming fluids (Kerrich, 1987).

The $\delta^{18}O$ values of vein quartz in the STGP (+11.5‰ to +13.5‰) coincide most closely with those of quartz from Proterozoic mesothermal deposits of the Slave and Churchill provinces, and also with those from Archean gold deposits in central and eastern Abitibi (summary by Kerrich, 1989a). The uniformity in $\delta^{18}O$ values of quartz, regardless of vein type or proximity to mineralization in the STGP, reflects a homogeneity in the ^{18}O content of the hydrothermal fluids, combined with an overall uniformity in the temperatures of vein formation.

The few carbonate analyses from the STGP yielded $\delta^{13}C$ values (-5.6‰ to -6.9‰) that coincide with values cited for the average crustal carbon (Ohmoto and Rye, 1979) and with those of the low ^{13}C members of Archean gold deposits (Kerrich, 1989a). The $\delta^{13}C$ values of ankerite overlap with the field of magmatic carbon (Valley, 1986), though values in this range are not generally considered unique indicators of magmatic, metamorphic, or sedimentary sources (Ohmoto and Rye, 1979).

Discussion

Structural Setting

Mesothermal gold deposits are characteristically associated with major geological structures that juxtapose terranes of contrasting nature in an accretionary tectonic setting (Kerrich and Wyman, 1990; Barley and Groves, 1992). On a local scale, gold occurrences are known to be concentrated along the second- or higher-order splays of such structures (Kerrich, 1989a). In north-central Newfoundland, the Baie Verte Line reflects a crustal-scale discontinuity with a complex history of fault movement, which has brought the accreted oceanic terranes of the Dunnage Zone into contact with the metamorphosed rocks of the ancient Laurentian continental margin (Fig. 1). The Scrape Thrust and its associated system of faults/shear zones branch off the Baie Verte Line near Baie Verte (Figs. 1 and 2) within an overall structural setting that reflects juxtaposition of ophiolitic assemblages (e.g., Point Rousse Complex) against the metasedimentary rocks of the Fleur de Lys Supergroup. In this context, the terrane boundary faults may have served as conduits for the advection of fluids from depth. Four of the main gold prospects on the Baie Verte Peninsula, including the Dorset (Belanger et al., 1994), Pine Cove (Scott et al., 1991), Deer Cove (Patey and Wilton, 1993), and the Stog'er Tight (this paper), together with a number of smaller showings, occur in association with the Scrape Thrust or its related shear zones.

Chemical Mass Balance and Elemental Mobility

Hydrothermal alteration in the STGP involved variable degrees of CO_2, S, LILE (K, Rb, and Ba) and/or Na metasomatism (Appendix 2). Since no appreciable, pre-existing carbonate or graphite is found in the unaltered wall rocks, the abundance of carbonate in the alteration zones attests to the extensive contribution of CO_2 from hydrothermal fluids in all stages of alteration. The same applies to S that was introduced predominantly from the ore-forming fluids and may comprise nearly 20 modal percent of the mineralized wall rock in the form of sulfide. Wall rock alteration by CO_2- and S- (also P-) rich hydrothermal fluids facilitated widespread elemental mobility at the STGP.

The concentrations of K and Rb increase with alteration and reach about 40 times that of the precursor (or more) in the ankerite-sericite zone (Appendices 1 and 2). These enrichments are closely associated with the formation of hydrothermal sericite in the rock. Despite the strong K and Rb metasomatism, the K/Rb ratios of the altered rocks remain within the 400 to 600 range, consistent with those in the precursor gabbro. In contrast, the K/Ba ratios increase systematically with alteration by nearly an order of magnitude (from 30 to 270), mainly because of larger enrichment in K relative to Ba. The covariant relationships among the

LILE, as controlled by K-silicate precipitation and manifested in uniform K/Rb and K/Ba ratios, are considered by many workers as a characteristic feature of mesothermal gold deposits and have formed a basis for the metamorphic devolatilization model cited for the origin of mesothermal Au-bearing fluids (e.g., Kerrich, 1989a, 1989b). In this regard, the conspicuously elevated K/Ba ratios in the STGP somewhat deviate from the typical LILE behavior considered for the majority of mesothermal deposits, and seem to approach the chemical trends characteristic of the magmatic-hydrothermal systems (Kerrich, 1989a and references therein). Sodium metasomatism is limited to albite precipitation in the red albite-pyrite zone and is significantly smaller in magnitude in comparison to the LILE enrichments.

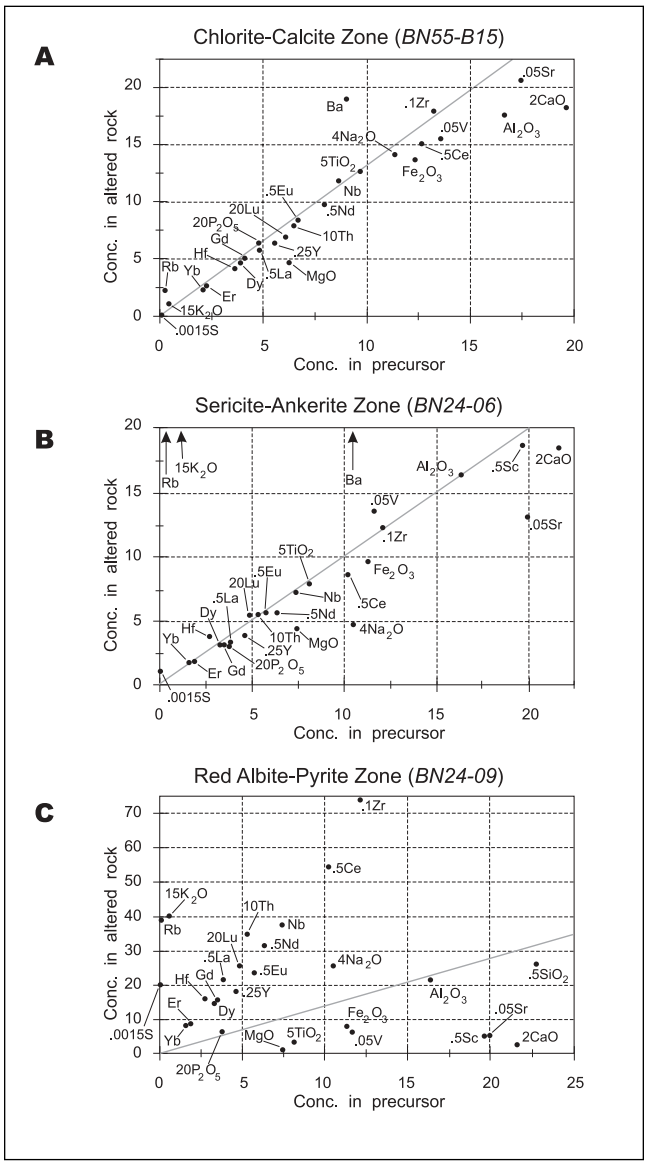

Fig. 6. Isocon diagrams for three representative samples of the main alteration assemblages plotted against the composition of precursor gabbro in the corresponding drill hole. Only the key elements are plotted and their concentrations are scaled proportionally for clarity. Precursor (unaltered) gabbro is represented by samples BN55-B12 for (A) and BN24-01 for (B) and (C). See Appendices 1 and 2 for compositional data.

The elevated concentrations of REE, HFSE, and Th in the red albite-pyrite and chlorite-magnetite zones of the STGP exceed the range of compositions of most of the samples of the precursor gabbro (Fig. 4B, drill hole 24) and thus cannot be explained by primary magmatic processes. Hydrothermal fluid-rock reactions are likely to have been responsible for the observed trace element enrichments. Decoupling among the REE, Zr, and P_2O_5 (also LILE) concentrations in the altered rocks (Fig. 4B), as opposed to their systematic, fractionation-controlled covariations in the precursor gabbro, further corroborates the above conclusion. Substantial enrichments in the REE, HFSE, and Th by fluid-rock reaction are somewhat enigmatic, as these are generally presumed to be the least mobile trace elements during hydrothermal alteration (e.g., Pearce and Cann, 1973) and hence variations in their absolute abundances have been commonly attributed to the alteration-related changes in total mass (i.e., isochemical behavior; Kerrich, 1989b). The abundance of REE-bearing hydrothermal phases, such as apatite, zircon, monazite and xenotime, in the alteration zones of the STGP clearly contradicts the assumption of immobility. Mass balance considerations are nevertheless required to account for possible compositional changes due to bulk gains or losses in mass (or volume). Note that the chlorite-magnetite zone is not discussed in this context. This zone has been interpreted to have a complex, multi-episodic style of alteration, as evidenced by its alteration overprint textures (see *Alteration Mineralogy and Zonation*).

The isocon scheme of Grant (1986) was used in this paper as a direct method of solving the conventional Gresens' (1967) equations for composition-volume changes. In the isocon method, the elemental concentrations in the altered rock are plotted against those in the precursor and a straight line (isocon), whose slope is proportional to the net change of mass, is defined graphically by connecting points corresponding to elements of isochemical character (Fig. 6). The composition of the altered rock can then be reconstituted by correcting for the calculated gain or loss in mass (Appendix 2) and the volume-independent chemical changes can be estimated (Fig. 7). It is apparent that the net mass change (slope of isocon) would depend on the choice of isochemical components. The least mobile components used in our mass balance calculations include variable combinations of Al_2O_3, TiO_2, P_2O_5, Zr, Nb, and Y. The unaltered gabbro composition from the same drill-core was selected as the precursor for each calculation. The isocon is selected carefully in each case such that the overall gains and losses in rock components would be consistent with the observed alteration mineralogy.

In the case of the red albite-pyrite zone, a best-fit line through the REE data points would result in losses of 50% for Na_2O and 75% or more for each other major oxides relative to the precursor (Fig. 6C), which are clearly in conflict with the albite-rich assemblage of the rock. Therefore, the

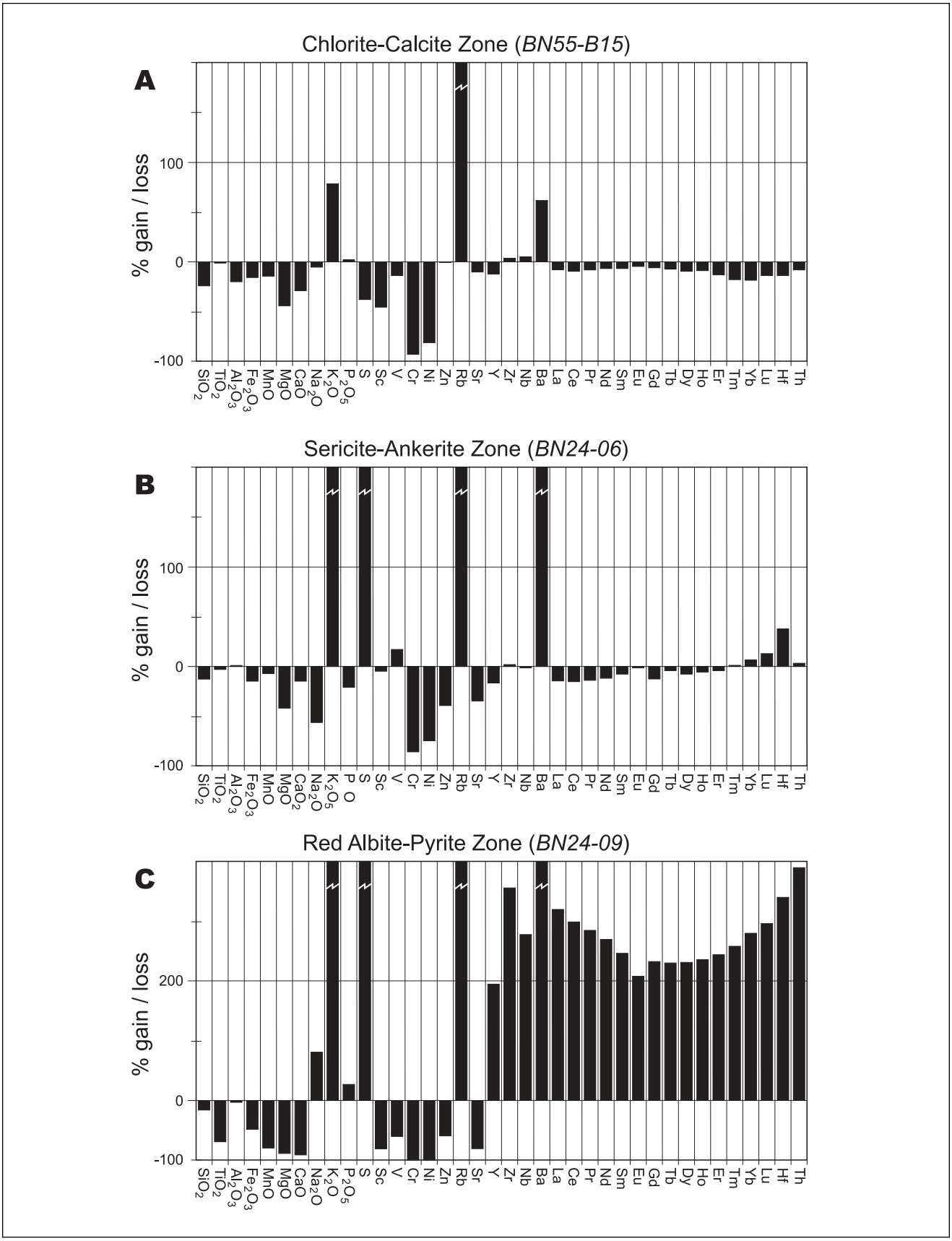

Fig. 7. Elemental gains and losses for representative samples of alteration assemblages in the Stog'er Tight prospect, based on isocon calculations (Fig. 6) and the corresponding data corrections for net changes in mass (Appendix 2). Broken bars indicate enrichments beyond the scale of the diagram. Note that scale is different in C.

REE are interpreted not to have remained isochemical and an excess of the REE must have been introduced into the rock during fluid-rock reaction (Figs. 6C and 7C). It must be noted that the isocon of Figure 6C presents a hypothetical solution to the net changes of mass in the red albite-pyrite zone while the geochemical complexities of this zone should by no means be de-emphasized.

The REE in the red albite-pyrite zone (sample BN24-09) were not enriched uniformly, but rather the LREE and the HREE were systematically more enriched (300%) relative to the MREE (230%). Thorium, Zr, and Nb are enriched by factors of 3.9, 3.5, and 2.8, respectively (Fig. 7C). The lack of correlation between enrichments in P_2O_5 (26%) and in the REE suggests that the observed enrichment trends are more likely to have been controlled by the hydrothermal precipitation of zircon (and other REE-bearing silicates), rather than by the formation of hydrothermal phosphates such as apatite and monazite. In contrast, samples from both the chlorite-calcite zone and the sericite-ankerite zone are slightly depleted in the majority of REE (and Y) relative to the precursor gabbro (Figs. 7A, 7B). This suggests that at least part of the excess REE in the red albite-pyrite zone might have been supplied by the alteration-induced leaching of trace elements away from the surrounding, less intensely altered rocks. A similar process of internal redistribution of REE (and HFSE) on a small scale by Au-bearing fluids has been observed by Ludden et al. (1984) in connection to gold mineralization in the Val d'Or camp in Quebec. Nevertheless, REE depletions in the lesser altered rocks of the STGP are generally small (<20%) and lie within the range of uncertainty associated with the mass balance calculations. As in the Val d'Or deposits, the unequivocal existence of an external or internal source for the REE in the STGP has proven difficult to evaluate.

Host Rock Control on Mineralization

Gold mineralization in the STGP is structurally controlled by a network of shear zones which is best developed in the gabbro sills. Shear deformation is viewed to be genetically related to south-verging displacements along the Scrape Thrust, in accord with strike-slip movements along the Baie Verte Line. The close association of gold mineralization with shear deformation and hydrothermal alteration which has overprinted the greenschist facies assemblage of the gabbro, is indicative of an epigenetic, but largely stratabound, style of mineralization. Alteration was only locally developed in the volcanic sequence and no mineralization has been observed beyond the margins of gabbro. Shear zones, as channels for fluid percolation and fluid-rock reaction, were preferentially developed in the gabbro, evidently because of its favorable rheology (e.g., isotropic fabric or rigidity). In addition to its mechanical role, gabbro served as a chemical sink for gold mineralization. Chemical reaction between Fe-Ti oxide phases (ilmenomagnetite) from the gabbro and the hydrothermal fluid containing soluble gold-sulfur complexes induced the oxidation (de-sulfidation) of fluid and resulted in the co-precipitation of pyrite and gold inside the altered wall rock. The abundance of rutile-rich leucoxene in the mineralized gabbro, and its direct textural association with gold-bearing pyrite, provide strong evidence for a model of gold precipitation by fluid-rock reaction. Considering that gold is likely to be transported in the hydrothermal fluid predominantly in the form of the neutral hydrosulfide complex, $AuHS^0$ [or as $AuHS(H_2S)_3^0$ at pressures above 100 MPa as suggested by Loucks and Mavrogenes (1999)] over the temperatures of interest (Benning and Seward, 1996; Gibert et al., 1998), the mineralization reaction can be formulated as:

$$\underset{\text{(ilmenite)}}{FeTiO_3} + 2\mathbf{Au}HS^0 \rightarrow \underset{\text{(pyrite)}}{FeS_2} + \underset{\text{(rutile)}}{TiO_2} + 2\mathbf{Au}_{(s)} + H_2O_{(aq)}$$

It should be noted that despite the strong ore-gabbro association in the STGP, other gold occurrences associated with the Baie Verte Line are hosted by a variety of rock types. These include mafic volcanic/volcaniclastic rocks at Deer Cove (Dubé et al., 1993), mafic tuffs at Pine Cove (Scott et al., 1991), and felsic porphyry dikes at Hammer Down (Ritcey et al., 1995). In the great majority of these occurrences, gold mineralization occurs predominantly in quartz-rich veins, suggesting mechanisms other than, or in addition to, fluid-rock reaction for the precipitation of gold.

Recent experimental data for Au solubility in supercritical aqueous fluids (Gibert et al., 1998; Loucks and Mavrogenes, 1999) have demonstrated that cooling and/or decompression associated with fluid migration from amphibolite to greenschist facies conditions (or equivalent conditions in the vicinity of epizonal plutons) alone may cause a drastic decrease in the solubility of gold-sulfur complexes. These may help to explain the multiple mechanisms controlling gold precipitation throughout an area such as the Baie Verte Peninsula.

Regional Aspects of Gold Mineralization

The shallow-level gabbro sills of the STGP lack the magmatic-arc chemical signature characteristic of their host basaltic-andesitic volcanic rocks. The enriched (E-type) MORB affinity of the main Stog'er Tight gabbro is interpreted to represent late-stage tholeiitic magmatism associated with arc rifting, and possibly back-arc basin development, prior to the Early Ordovician (Taconian) emplacement (Dallmeyer and Williams, 1975; Dunning and Krogh, 1985) of oceanic allochthons onto the Laurentian margin. The measured 483 +3/-2 Ma age of the Stog'er Tight gabbro is similar to the Middle Arenigian (Ordovician) fossil age of the Snooks Arm Group (Snelgrove, 1931) that covers the Betts Cove ophiolite complex to the southeast (Fig. 1) and is also host to the Nugget Pond gold mine (Swinden et al.,

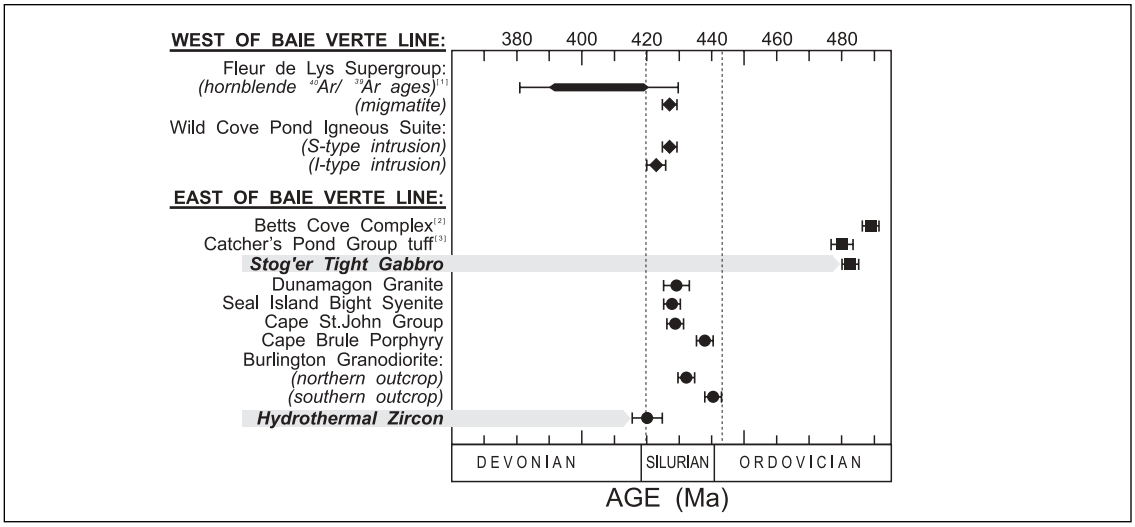

Fig. 8. Compilation of isotopic ages from the Baie Verte Peninsula, including the host gabbro and hydrothermal zircon ages from the Stog'er Tight prospect (highlighted). All age data are from Cawood and Dunning (1993) unless noted otherwise; [1] Dallmeyer (1977) recalculated to new Ar decay constants, [2] Dunning and Krogh (1985), [3] Ritcey et al. (1995). Time scale incorporates recent calibrations of Tucker et al. (1990) and Bowring et al. (1993).

1990). The Betts Cove Complex is correlated with the main body of the Point Rousse Complex (Hibbard, 1983) and its Early Ordovician age of 488.6 +3.1/-1.8 Ma (Dunning and Krogh, 1985) corroborates the suggested stratigraphic correlations.

The Late Silurian age of hydrothermal zircon (420 ±5 Ma) from the red albite-pyrite zone is consistent with the epigenetic style of mineralization in the STGP and implies that hydrothermal alteration, and hence gold mineralization, post-dated the intrusion of host gabbro by about 63 Ma. Relict hydrothermal zircon is also found in the chlorite-magnetite altered gabbro, which bears evidence for late- to post-ore (overprint) alteration and cataclastic deformation. This further supports the conclusion that zircon and gold co-precipitated at the peak of hydrothermal (red albite-pyrite) alteration in the Late Silurian.

Abundant high-precision isotopic ages from north-central Newfoundland have made it possible to put the gold mineralization event in the STGP into a regional chronologic perspective (Fig. 8). The U-Pb ages of I-type granitoid intrusions and felsic volcanic rocks from the Dunnage Zone on the Baie Verte Peninsula (Cawood and Dunning, 1993) lie within a narrow range in the Silurian (ca. 440 Ma to 424 Ma). Peak metamorphism of the continental margin rocks of the Humber Zone on the Baie Verte Peninsula (Jamieson, 1990) is constrained by U-Pb dates from migmatites of the Fleur de Lys Supergroup (Cawood and Dunning, 1993), and also $^{40}Ar/^{39}Ar$ ages from metamorphic hornblende (Dallmeyer, 1977) to have a similar Silurian age. The age of post-kinematic, I-type granitoid intrusion into the continental margin (423 ±3 Ma, Cawood and Dunning, 1993), in particular, overlaps within uncertainty with that of the hydrothermal zircon from the STGP. These ages are consistent with a model of post-peak metamorphic, late-magmatic, mesothermal gold mineralization that took place during the waning stages of Silurian Orogeny on the Baie Verte Peninsula. Similar temporal relationships characterize primary gold mineralization resulting from accretion of allochthonous terranes in mesothermal deposits of various ages (Kerrich and Wyman, 1990; Kerrich and Cassidy, 1994), including those in the Val d'Or district of the Archean Abitibi greenstone belt in Quebec (Kerrich and Kyser, 1994), Archean Yilgarn Craton of Western Australia (Kent et al., 1996), Paleozoic Meguma terrane of the Canadian Appalachians (Kontak et al., 1990) and the Mesozoic-Cenozoic Juneau gold belt of Alaska (Goldfarb et al., 1991; Miller et al., 1994). The short time lapse between peak metamorphic-magmatic events and gold mineralization on the Baie Verte Peninsula is clearly in contrast with the model of post-metamorphic, post-magmatic ("late") gold deposition that predicts a ca. 100 Ma gap preceding gold mineralization as the result of diachronous metamorphism or delayed thermal equilibration in a tectonically thickened crust (e.g., Jemielita et al., 1990; Hanes et al., 1992).

In the absence of robust evidence for the source(s) of the Au-bearing fluids, the Silurian mantle-derived magmatism, regional metamorphism and anatectic melting of the continental margin rocks each could have plausibly contributed to the hydrothermal activity on the Baie Verte Peninsula. This could have been achieved either by direct emanation of magmatic volatiles, or by igneous activity supplying the thermal energy for rock dehydration and fluid advection through the overlying crust. Considering the mesothermal style of alteration, the ore paragenesis (high Au/Ag ratio and insignificant Sb, As, and Bi), and the oxygen isotope composition of the ore fluids at the STGP, meteoric waters are unlikely to have been a principal fluid source. Three end-member sources can be conceived for the ore fluids and their solutes: 1) metaclastic-metapelitic, continental margin rocks of the Fleur de Lys Supergroup, 2) accreted

ophiolitic and oceanic, mafic volcanic-epiclastic rocks, and 3) Silurian magmatic intrusions.

The extensive hydrothermal alteration in the STGP, reaching tens of meters in thickness and involving intensive LILE, REE and HFSE metasomatism, suggests prior chemical equilibration of the fluids with rocks significantly different in composition than the host oceanic mafic (or ultramafic) rocks. It has also been demonstrated that the ophiolite-hosted auriferous veins throughout the Baie Verte Peninsula bear a mantle-like strontium isotopic signature ($^{87}Sr/^{86}Sr \simeq 0.705$ to 0.706) that is in contrast with the more radiogenic strontium ($^{87}Sr/^{86}Sr \simeq 0.720$) measured from similar veins in the Laurentian basement (Wilson et al., 1994). The trace element and Sr isotopic evidence appear to rule out the possibilities (a) and (b) above, suggesting that the Silurian I-type intrusions are the most viable source for the Au-bearing fluids in the STGP.

The LILE systematics (e.g., elevated K/Ba ratios) and the stable isotope thermometry from the STGP, though inconclusive, support an orthomagmatic fluid reservoir. There has been increasing evidence for the involvement of juvenile magmatic fluids in the genesis of high temperature, high Au/Ag-Sb-Hg, mesothermal gold deposits worldwide (e.g., McCuaig and Kerrich, 1998), though their role as the dominant reservoir for ore fluids remains a matter of debate.

The Appalachian Gold Dilemma

The Appalachian orogeny was associated with an accretionary tectonic regime, involving oceanic 'greenstone' terranes, and a large-scale hydrothermal plumbing system during the Silurian (Cawood et al., 1994; Wilson et al., 1994) that could provide favorable conditions for shear-hosted gold mineralization. It is not entirely understood why the Northern Appalachian accreted terranes appear not to have produced economic deposits comparable to world-class examples found in large gold provinces of similar geologic setting (e.g., the Archean Abitibi greenstone belt).

Phillips et al. (1996) suggested that the formation of giant gold deposits, such as Kalgoorlie, Western Australia, and Timmins, Canada, depends on the probability of all of the principal parameters in the ore-forming process (e.g., high heat flow, large fluid reservoir, efficient fluid focussing, mechanically and chemically favorable host rocks) reaching their optimum magnitudes, rather than on any particular parameter(s) alone. Accordingly, the small scale of gold mineralization in Newfoundland may be attributed to such factors as the low Au concentration of the source rocks or the limited distribution of suitable host rocks along the sites of major shear deformation. On the deposit scale, the STGP does not bear evidence of recurrent deformation and fluid flow or episodic brittle to ductile transition, such as cross-cutting or banded (ore-stage) quartz veins. This may imply that the duration of Silurian magmatic and metamorphic events was too short to allow sustained hydrothermal activity and continued mineralization over a significant period of geologic time.

It has been suggested that internal orogens (involving continent-continent collision), such as the Trans-Hudson, Appalachian and Alpine belts, generally do not feature large mesothermal gold provinces. This is possibly because of shallower and less interconnected structural networks along the internal orogens, in contrast to the deeper and more extensive plumbing systems developed along the boundaries of accreted terranes in external orogens (McCuaig and Kerrich, 1998). It may also be related to the episodic nature of orogenesis, deformation, and hydrothermal activity associated with continued terrane accretion in external orogens, which takes place over an extended period of time. An alternative (and optimistic) explanation for the lack of large gold deposits in the accreted oceanic terranes of Newfoundland may be that the deep-seated, ductile, crustal structures, recognized as the hosts of mesothermal gold deposits elsewhere, have not been widely exposed at the surface throughout the northern Appalachians. In other words, the gold occurrences of north-central Newfoundland may represent merely the "tips of the iceberg" compared to the mineralized structures that may lie at greater crustal depths. Although no strong evidence is currently in hand to support the latter hypothesis, further targeted geologic research and exploration may yet provide a more compelling solution to the Appalachian gold problem.

Conclusions

The Stog'er Tight gold prospect is an epigenetic, shear-hosted gold deposit that is hosted by shallow-level gabbro sills within an Ordovician volcanic arc/back-arc sequence in north-central Newfoundland. Its hydrothermal alteration assemblage and style of mineralization is typical of a high-temperature, mesothermal gold deposit, including a gangue mineralogy dominated by albite, pyrite, ankerite, sericite, chlorite, and quartz. Deformation associated with mineralization was driven by displacement along a regional terrane boundary suture, the Baie Verte Line, in an accretionary tectonic setting. Gold occurs with pyrite, inside strongly altered gabbro at the margins of syn-deformational, quartz-rich veins. Fluid-wall rock reaction involving Fe-bearing oxides and silicates in the gabbro led to the precipitation of pyrite and gold by oxidation of ore-bearing fluid and de-stabilization of soluble gold hydrosulfide complexes.

Wall rock alteration in the Stog'er Tight prospect features elevated REE, HFSE, and Th concentrations, in addition to CO_2, LILE, S, and Na metasomatism characteristic of most greenstone-hosted mesothermal gold deposits. A rare, hydrothermal variety of zircon from the high-grade ore zone at Stog'er Tight yielded a U-Pb age of 420 ± 5 Ma for the mineralization event. Gold was deposited near the final stage of a Silurian period of regional metamorphism and orogenic magmatism that involved both the continental basement and the accreted oceanic terranes. Our age, geo-

chemical and stable isotopic results, together with other available data, collectively support a model of late-magmatic gold mineralization involving fluids that were derived at least in part from the Silurian I-type plutons.

Acknowledgments

This work resulted for the most part from J.R.'s M.Sc. dissertation that was supported logistically and financially by the Noranda Exploration Co. Ltd. Al Huard (Noranda) is thanked for his insightful information and access to unpublished data. Additional financial support was received from a Memorial University graduate fellowship to J.R. and Natural Sciences and Engineering Council research grants to G.R.D. and M.R.W. The stable isotope analyses were performed in part by Adrian Timbal. We are grateful to Benoit Bubé and Peter Cawood for helpful advice in the field. Tom Setterfield is thanked for his thorough review of the manuscript.

References

BARLEY, M.E. and GROVES, D.I., 1992. Supercontinent cycles and the distribution of metal deposits through time. Geology, 20, p. 291-294.

BARLEY, M.E., EISENLOHR, B.N., GROVES, D.I., PERRING, G.S. and VEARNCOMBE, J.R., 1989. Late Archean convergent margin tectonics and gold mineralization. A new look at the Norseman-Wiluna belt, Western Australia. Geology, 17, p. 826-829.

BELANGER, M., DUBÉ, B., LAUZIÉRE, K. and MALO, M., 1994. Geology of the mesothermal Dorset gold showing, Baie Verte Peninsula, Newfoundland. Report of Activities, Newfoundland Geological Survey Branch, p. 55-56.

BENNING, L.G. and SEWARD T.M., 1996, Hydrosulphide complexing of Au(I) in hydrothermal solutions from 150-400°C and 500-1500 bar. Geochimica et Cosmochimica Acta, 60, p. 1849-1871.

BOWRING, S.A., GROTZINGER, J.P., ISACHSEN, C.E., KNOLL, A.H., PELECHATY, S.M. and KOLOSOV, P., 1993. Calibrating rates of early Cambrian evolution. Science, 261, p. 1293-1298.

CAWOOD, P.A. and DUNNING, G.R., 1993. Silurian age for movement on the Baie Verte Line: Implications for accretionary tectonics in the northern Appalachians. Geological Society of America Program with Abstracts, p. A-422.

CAWOOD, P.A., DUNNING, G.R., LUX, D. and VAN GOOL, J.A.M., 1994. Timing of peak metamorphism and deformation along the Appalachian margin of Laurentia in Newfoundland: Silurian and not Ordovician. Geology, 22, p. 399-402.

CLAYTON, R.N. and KIEFFER, S.W., 1991. Oxygen isotopic thermometer calibrations. *In* Stable Isotope Geochemistry; A tribute to Samuel Epstein. *Edited by* H.P. Taylor, Jr., J.R. O'Neil and I. R. Kaplan. Geochemical Society Special Publication 3, p. 3-10.

CLAYTON, R.N. and MAYEDA, T.K., 1963. The use of bromine pentafluoride in the extraction of oxygen from oxides and silicates for isotopic analysis. Geochimica et Cosmochimica Acta, 27, p. 43-52.

DALLMEYER, R.D., 1977. $^{40}Ar/^{39}Ar$ age spectra of minerals from the Fleur de Lys Terrane in Northwest Newfoundland: Their bearing on chronology of metamorphism within the Appalachian Orthotectonic Zone. Journal of Geology, 85, p. 89-103.

DALLMEYER, R.D. and WILLIAMS, H., 1975. $^{40}Ar/^{39}Ar$ ages from the Bay of Islands metamorphic aureole: Their bearing on the timing of Ordovician ophiolite abduction. Canadian Journal of Earth Sciences, 12, p. 1685-1690.

DAVIS, D.W., 1982. Optimum linear regression and error estimation applied to U-Pb data. Canadian Journal of Earth Sciences, 19, p. 2141-2149.

DUBÉ, B., 1990. A preliminary report on contrasting structural styles of gold-only deposits in western Newfoundland. Geological Survey of Canada, Paper 90-1B, p. 77-90.

DUBÉ, B., LAUZIÉRE, K. and POULSEN, H.K,, 1993. The Deer Cove deposit: An example of "thrust"-related breccia-vein type gold mineralization in the Baie Verte Peninsula, Newfoundland. Current Research, Geological Survey of Canada, Paper 93-ID, p. 1-10.

DUBÉ, B., DUNNING, G.R., LAUZIÉRE, K. and RODDICK, J.C., 1996. New insights into the Appalachian Orogen from geology and geochronology along the Cape Ray fault zone, southwest Newfoundland. Geological Society of America Bulletin, 108, p. 101-116.

DUNNING, G.R. and KROGH, T.E., 1985. Geochronology of ophiolites of the Newfoundland Appalachians. Canadian Journal of Earth Sciences, 22, p. 1659-1670.

DUNNING, G.R., O'BRIEN, S.J., COLMAN-SADD, S.P., BLACKWOOD, R.F., DICKSON, W.L., O'NEILL, P.P. and KROGH, T.E., 1990. Silurian Orogeny in the Newfoundland Appalachians. Journal of Geology, 98, p. 895-913.

GIBERT, F., PASCAL, M.-L. and PICHAVANT, M., 1998. Gold solubility and speciation in hydrothermal solutions: Experimental study of the stability of hydrosulphide complex of gold ($AuHS^0$) at 350 to 450°C and 500 bars. Geochimica et Cosmochimica Acta, 62, p. 2931-2947.

GOLDFARB, R.J., SNEE, L.W., MILLER, L.D. and NEWBERRY, R.J., 1991. Rapid dewatering of the crust deduced from ages of mesothermal gold deposits. Nature, 354, p. 296-298.

GRANT, J.A., 1986. The isocon diagram — A simple solution to Gresens' equation for metasomatic alteration. Economic Geology, 81, p. 1976-1982.

GRESENS, R.L., 1967. Composition-volume relationships of metasomatism. Chemical Geology, 2, p. 47-55.

HANES, J.A., ARCHIBALD, D.A., HODGSON, C.J. and ROBERT, F., 1992. Dating of Archean auriferous quartz vein deposits in the Abitibi greenstone belt, Canada, $^{40}Ar/^{39}Ar$ evidence for a 70- to 100-m.y. time gap between plutonism-metamorphism and mineralization. Economic Geology, 87, p. 1849-1861.

HIBBARD, J., 1983. Geology of the Baie Verte Peninsula, Newfoundland, Newfoundland Department of Mines and Energy, Memoir 2, 279 p.

HODGSON, C.J., HAMILTON, J.V., HANES, J.A. and PIROSHCO, D.W., 1990. Late emplacement of gold in the Archean Abitibi and analogous Phanerozoic "greenstone" belts: A consequence of thermal equilibration following collisional orogeny. *In* Greenstone Gold and Crustal Evolution. *Edited by* F. Robert, P.A. Sheahan and S.B. Green. Geological Association of Canada Nuna Conference Volume, p. 171.

HUARD, A.A., 1990. The Noranda/Impala Stog'er Tight deposit. International Association on the Genesis of Ore Deposits, 8th Symposium, Field Trip Guide, p. 173-177.

HUTCHINSON, R.W., 1987. Metallogeny of Precambrian gold deposits: Space and time relationships. Economic Geology, 82, p. 1993-2007.

JAMIESON, R.A., 1990. Metamorphism of an Early Paleozoic continental margin, Western Baie Verte Peninsula, Newfoundland. Journal of Metamorphic Geology, 8, p. 269-288.

JEMIELITA, R.A., DAVIS, D.W. and KROGH, T.E., 1990. U-Pb evidence for Abitibi gold mineralization postdating greenstone magmatism and metamorphism. Nature, 346, p. 831-834.

JENNER, G.A. and FRYER, B.J., 1980. Geochemistry of the Upper Snooks Arm Group basalts, Burlington Peninsula, Newfoundland: Evidence against formation in an island arc. Canadian Journal of Earth Sciences, 17, p. 888-900.

KEAN, B.F. and EVANS, D.T.W., 1987. King's Point, Newfoundland (12H/9). Government of Newfoundland and Labrador, Department of Mines and Energy, Map 87-06.

KEAYS, R.R. and SKINNER, B.J., 1989. Introduction. *In* The Geology of Gold Deposits: The Perspective in 1988. *Edited by* R.R. Keays, R.H. Ramsay and D.I Groves. Economic Geology Monograph 6, p. 1-8.

KENT, A.J.R., CASSIDY, K.F. and FANNING, C.M., 1996. Archean gold mineralization synchronous with the final stages of cratonization, Yilgarn Craton, Western Australia. Geology, 24, p. 879-882.

KERRICH, R., 1987. The stable isotope geochemistry of Au-Ag vein deposits in metamorphic rocks. *In* Stable Isotope Geochemistry of Low Temperature Fluids. *Edited by* T.K. Kyser. Mineralogical Association of Canada Short Course Notes, 13, p. 287-336.

KERRICH, R., 1989a. Geodynamic setting and hydraulic regimes: Shear zone hosted mesothermal gold deposits. *In* Mineralization and Shear Zones. *Edited by* J.T. Bursnall. Geological Association of Canada Short Course Notes, 6, p. 89-128.

KERRICH, R., 1989b. Lithophile element systematics of gold vein deposits in Archean greenstone belts: Implications for source processes. *In* The Geology of Gold Deposits: The Perspective in 1988. *Edited by* R.R., Keays, W.R.H. Ramsay and D.I. Groves. Economic Geology, Monograph 6, p. 508-520.

KERRICH, R. and CASSIDY, K.F., 1994. Temporal relationships of gold mineralization to accretion, magmatism, metamorphism and deformation — Archean to present: A review. Ore Geology Reviews, 9, p. 263-310.

KERRICH, R. and KYSER, T.K., 1994. 100 Ma timing paradox of Archean gold, Abitibi greenstone belt (Canada): New evidence from U-Pb and Pb-Pb evaporation ages of hydrothermal zircons. Geology, 22, p. 1131-1134.

KERRICH, R. and WYMAN, D., 1990. Geodynamic setting of mesothermal gold deposits; an association with accretionary tectonic regimes. Geology, 18, p. 882-885.

KIDD, W.S.F., DEWEY, J.F. and BIRD, J.M., 1978. The Ming's Bight Ophiolite Complex, Newfoundland: Appalachian oceanic crust and mantle. Canadian Journal of Earth Sciences, 15, p. 781-804.

KIRKWOOD, D. and DUBÉ, B., 1992. Structural control of sill-hosted gold mineralization: The Stog'er Tight Gold Deposit, Baie Verte Peninsula, Northwestern Newfoundland. Current Research, Geological Survey of Canada, 92-1D, p. 211-221.

KONTAK, D.J., SMITH, P.K., KERRICH, R. and WILLIAMS, P.F., 1990. Integrated model for Meguma Group lode gold deposits, Nova Scotia, Canada. Geology, 18, p. 238-242.

KROGH, T.E., 1973. A low-contamination method for hydrothermal decomposition of zircon and extraction of U and Pb for isotopic age determination. Geochimica et Cosmochimica Acta, 37, p. 488-494.

KROGH, T.E., 1982a. Improved accuracy of U-Pb zircon ages by the creation of more concordant systems using an air abrasion technique. Geochimica et Cosmochimica Acta, 46, p. 637-649.

KROGH, T.E., 1982b. Improved accuracy of U-Pb zircon dating by selection of more concordant fractions using a high gradient magnetic separation technique. Geochimica et Cosmochimica Acta, 46, p. 631-635.

LONGERICH, H.P., JENNER, G.A., FRYER, B.J. and JACKSON, S.E., 1990. Inductively coupled plasma-mass spectrometric analysis of geological samples: A critical evaluation based on case studies. Chemical Geology, 83, p. 105-118.

LOUCKS, R.R. and MAVROGENES, J.A., 1999. Gold solubility in supercritical hydrothermal brines measured in synthetic fluid inclusions. Science, 284, p. 2159-2163.

LUDDEN, J.N., DAIGNEAULT, R., ROBERT, F. and TAYLOR, R.P., 1984. Trace element mobility in alteration zones associated with Archean Au lode deposits. Economic Geology, 79, p. 1131-1141.

MATSUHISA, Y., GOLDSMITH, J.R. and CLAYTON, R.N., 1979. Oxygen isotopic fractionation in the system quartz-albite-anorthite-water. Geochimica et Cosmochimica Acta, 43, p. 1131-1140.

McCREA, J.M., 1950. On the isotope chemistry of carbonates and a paleotemperature scale. Journal of Chemical Physics, 18, p. 849-857.

McCUAIG, T.C. and KERRICH, R., 1998. P-T-t-deformation-fluid characteristics of lode gold deposits: Evidence from alteration systematics. Ore Geology Reviews, 12, p. 381-453.

McDONOUGH, W.F. and SUN, S.-S., 1995. The composition of the Earth. Chemical Geology, 120, p. 223-253.

MERCER, B., STRONG, D.F., WILTON, D.H.C. and GIBBONS, D., 1985. The King's Point Complex, western Newfoundland. Canada Geological Survey Paper 85-lA, p. 737-741.

MILLER, L.D., GOLDFARB, R.J., GEHRELS, G.E. and SNEE, L.W., 1994. Genetic links among fluid cycling, vein formation, regional deformation, and plutonism in the Juneau gold belt, southeastern Alaska. Geology, 22, p. 203-206.

NORMAN, R.E. and STRONG, D.F., 1975. The geology and geochemistry of ophiolitic rocks exposed at Ming's Bight, Newfoundland. Canadian Journal of Earth Sciences, 12, p. 777-797.

OHMOTO, H. and RYE, R.O., 1979. Isotopes of sulphur and carbon. *In* The Geochemistry of Hydrothermal Ore Deposits. *Edited by* H.L. Barnes. John Wiley and Sons, New York, p. 509-567.

O'NEIL, J.R. and TAYLOR, H.P., JR., 1969. Oxygen isotope equilibrium between muscovite and water. Journal of Geophysical Research, 74, p. 6012-6022.

PATEY, K.S. and WILTON, D.H.C., 1993. The Deer Cove Deposit, Baie Verte Peninsula, Newfoundland, a Paleozoic mesothermal lode-gold occurrence in the Northern Appalachians. Canadian Journal of Earth Sciences, 30, p. 1532-1546.

PEARCE, J.A. and CANN, J.R., 1973. Tectonic setting of basic volcanic rocks determined using trace element analyses. Earth and Planetary Science Letters, 19, p. 290-300.

PHILLIPS, G.N., GROVES, D.I. and KERRICH, R., 1996. Factors in the formation of the giant Kalgoorlie gold deposit. Ore Geology Reviews, 10, p. 295-317.

RAMEZANI, J., 1993. The Geology, Geochemistry and U-Pb Geochronology of the Stog'er Tight Gold Prospect, Baie Verte Peninsula, Newfoundland. M.Sc. thesis, Memorial University of Newfoundland, St. John's, Newfoundland, 312 p.

RITCEY, D.H., WILSON, M.R. and DUNNING, G.R., 1995. Gold mineralization in the Paleozoic Appalachian Orogen. Constraints from geologic, U/Pb, and stable isotope studies of the Hammer Down Prospect, Newfoundland. Economic Geology, 90, p. 1955-1965.

SCOTT, W.J., DIMMELL, P.M. and SCOTT, S.A., 1991. Induced polarization anomalies associated with auriferous zones, Pine Cove property, Baie Verte Area, Newfoundland. Geological Association of Canada, Program with Abstracts, 16, p. A-113.

SHEPPARD, S.M.F., NIELSEN, R.L. and TAYLOR, H.P., JR., 1969. Oxygen and hydrogen isotope ratios of clay minerals from porphyry copper deposits. Economic Geology, 64, p. 755-777.

SNELGROVE, A.K., 1931. Geology and ore deposits of Betts Cove-Tilt Cove area, Notre Dame Bay, Newfoundland. Canadian Mining and Metallurgical Bulletin, 228, p. 477-519.

STACEY, J.S. and KRAMERS, J.D., 1975. Approximation of terrestrial lead isotope evolution by a two-stage model. Earth and Planetary Science Letters, 26, p. 207-221.

SUN, S.-S. and McDONOUGH, W.F., 1989. Chemical and isotopic systematics of oceanic basalts, implications for mantle composition and processes. *In* Magmatism in the Ocean Basins. *Edited by* A.D. Saunders and M.J. Norry. Geological Society Special Publication 42, p. 313-345.

SWINDEN, S., McBRIDE, D. and DUBÉ, B., 1990. Preliminary geological and mineralogical notes on the Nugget Pond gold deposit, Baie Verte Peninsula, Newfoundland. Current Research, Newfoundland Department of Mines and Energy Report of Activities, Mineral Development Division, p. 201-215.

TUACH, J., DEAN, P.L., SWINDEN, H.S., O'DRISCOLL, C.F., KEAN, B.F. and EVANS, D.T.W., 1988. Gold mineralization in Newfoundland: A 1988 review. Current Research, Newfoundland Department of Mines and Energy, Report 88-1.

TUCKER, R.D., KROGH, T.E., ROSS, R.J. and WILLIAMS, S.H., 1990. Time-scale calibration by high-precision U-Pb zircon dating of interstratified volcanic ashes in the Ordovician and Lower Silurian stratotypes of Britain. Earth and Planetary Science Letters, 100, p. 51-58.

VALLEY, J.W., 1986. Stable isotope geochemistry of metamorphic rocks. *In* Stable Isotopes in High Temperature Geologic Processes. *Edited by* J.W. Valley, H.P. Taylor, Jr. and J.R O'Neil. Reviews in Mineralogy, 16, Mineralogical Society of America. Bookcrafters Inc., Michigan, p. 185-226.

WENNER, D.B. and TAYLOR, H.P., JR., 1971. Temperatures of serpentinization of ultramafic rocks based on $^{18}O/^{16}O$ fractionation between coexisting serpentine and magnetite. Contributions to Mineralogy and Petrology, 32, p. 165-185.

WILLIAMS, H., 1979, Appalachian Orogen in Canada. Canadian Journal of Earth Sciences, 16, p. 792-807.

WILLIAMS, H. and ST-JULIEN, P., 1982. The Baie Verte-Brompton Line. Early Paleozoic continental interface in the Canadian Appalachians. *In* Major Structural Zones and Faults of the Northern Appalachians. *Edited by* P. St-Julien and J. Beland. Geological Association of Canada, Special Paper 24, p. 177-207.

WILLIAMS, H. and STEVENS, R.K., 1974. The ancient continental margin of eastern North America. *In* The Geology of Continental Margins. *Edited by* C.A. Burk and C.L. Drake. Springer-Verlag, New York, p. 781-796.

WILSON, M.R., DUNNING, G.R. and CAWOOD, P.A., 1994. Fluid compositions in crustal-scale plumbing systems related to contrasting styles of Ordovician and Silurian orogenesis, Northern Appalachians, Newfoundland. Mineralogical Magazine, 58A, p. 977-978.

WOOD, D.A., JORON, J.L. and TREUIL, M., 1979. A reappraisal of the use of trace elements to classify and discriminate between magma series erupted in different tectonic settings. Earth and Planetary Science Letters, 50, p. 326-336.

Appendix 1. Chemical Data for the Main Igneous Rocks, Stog'er Tight Prospect

Sample(*)	BN53-10	BN55-B12	BN24-01	91822-3	BN55-B1	BN55-B9	BN55-B5	BN53-01	BN53-25	BN54-B5	BN54-R	91821-A1
Rock Type	Gabbro	Gabbro	Gabbro	Gabbro	Gabbro	Gabbro	Gabbro	Vol. tuff	Mafic vol.	Pillow core	Mafic vol.	Mafic vol.
Suite(**)	MGAB	MGAB	MGAB	MGAB	LFTG	LFTG	LFTG	VPU	VPU	VPU	VPU	VPU
SiO_2[f]	45.70	45.25	45.55	45.55	46.90	49.40	39.88	54.30	53.80	53.15	47.44	46.70
TiO^2	1.61	1.94	1.63	1.74	1.43	1.35	1.18	1.06	0.93	0.97	0.53	0.49
Al_2O_3	16.20	16.63	16.37	12.37	17.46	16.67	12.89	16.60	13.60	15.83	12.19	10.56
Fe_2O_3[ff]	12.38	12.36	11.33	12.88	13.51	10.54	14.20	8.39	8.10	7.61	10.90	7.55
MnO	0.13	0.16	0.14	0.19	0.17	0.17	0.23	0.10	0.11	0.17	0.20	0.14
MgO	5.03	6.28	7.44	7.30	8.01	6.37	12.14	7.24	8.69	6.06	9.18	10.08
CaO	9.53	9.82	10.82	8.60	4.97	9.37	10.42	4.23	7.35	7.77	8.83	14.24
Na_2O	2.80	2.84	2.63	3.20	4.42	4.00	2.02	2.99	4.88	4.37	3.06	3.59
K_2O	0.310	0.030	0.040	0.218	0.120	0.390	0.123	2.420	0.040	0.100	0.053	0.167
P_2O_5	0.210	0.240	0.190	0.486	0.160	0.140	0.167	0.130	0.380	0.390	0.011	0.000
Total	93.90	95.55	96.14	92.52	97.15	98.40	93.25	97.45	97.87	96.42	92.39	93.52
Mg#	48.07	54.52	60.06	52.86	59.55	56.99	62.87	68.06	73.39	64.97	62.50	72.56
S[fff]	175	56	45	45	537	100	255	188	1112	264	85	44
Sc	44	40	39	32	43	44	44	20	23	17	33	35
V	313	272	233	229	297	239	302	136	174	165	323	217
Cr	88	262	581	20	349	205	208	175	553	292	31	338
Ni	24.7	56	95	14	75	42	52	73.2	219.6	127	26	60
Cu	17.1	28	29	80	44	41	45	30.1	90.9	30	39	60
Zn	78.3	68	59	76	79	72	87	56.4	43.9	64	152	37
Ga	6.2	11	13	25	10	6	23	ND	3.5	9	14	14
Rb	6.3	0.3	0.1	3	1.6	6.5	2	45.6	0.6	0.6	1	2
Sr	350	349	399	273	155	286	270	135	442	421	130	93
Ba	29	9	11	46	23	56	28	247	52	25	10	20
Y	22.8	22.3	18.5	40.0	24.8	21.9	28.5	18.5	15.1	15.4	13.0	10.9
Zr	146	132	121	255	100	86	117	128	176	140	27	23
Hf	4.07	3.65	2.74	6.34	2.52	2.61	3.34	3.22	3.89	3.63	0.92	0.91
Nb	8.8	8.6	7.4	17	3.9	3.4	5	6.6	8.5	9.4	1	1
Th	0.64	0.65	0.53	1.72	0.95	0.90	1.22	3.77	8.60	5.62	0.30	0.42
La	10.74	9.65	7.75	19.00	6.86	5.50	7.82	13.10	41.49	30.71	1.67	1.36
Ce	28.05	25.32	20.41	47.82	16.67	14.06	20.27	29.96	87.42	66.25	4.25	3.47
Pr	3.96	3.56	2.85	6.46	2.35	2.04	2.87	3.50	10.20	7.60	0.62	0.55
Nd	17.95	15.96	12.73	29.07	11.33	9.89	13.77	14.81	37.96	28.48	3.15	2.85
Sm	4.77	3.96	3.27	7.54	3.26	2.89	4.10	3.41	5.98	4.95	1.16	1.13
Eu	1.71	1.34	1.15	2.45	1.17	1.10	1.66	1.03	1.72	1.46	0.36	0.44
Gd	5.09	4.10	3.54	8.19	4.24	3.75	5.15	3.77	4.52	4.15	1.63	1.55
Tb	0.79	0.64	0.55	1.28	0.69	0.64	0.84	0.57	0.54	0.52	0.31	0.27
Dy	4.93	3.92	3.34	7.88	4.46	4.21	5.43	3.61	3.06	2.93	2.26	1.83
Ho	1.00	0.81	0.68	1.52	0.98	0.90	1.11	0.72	0.60	0.58	0.51	0.41
Er	2.75	2.29	1.89	4.42	2.79	2.60	3.25	2.05	1.53	1.63	1.57	1.27
Tm	0.40	0.34	0.26	0.61	0.40	0.37	0.47	0.30	0.22	0.23	0.24	0.17
Yb	2.49	2.13	1.60	3.95	2.47	2.53	3.02	1.83	1.40	1.43	1.70	1.22
Lu	0.37	0.31	0.24	0.58	0.38	0.39	0.46	0.28	0.20	0.22	0.27	0.18

Notes

* Sample numbers starting with BN are from drill-core, the following two digits correspond to drill-hole number (see Fig. 3 for locations). All others are trench or outcrop (surface) samples.

** MGAB = main gabbro, LFTG = low Fe-Ti gabbro, VPU = volcanic-pyroclastic unit.

f Major oxide concentrations in percent.

ff Total Fe measured as Fe_2O_3 after complete oxidation of iron by ignition.

fff Trace element concentrations in parts per million.

ND = not detected, Vol. = volcanic.

Appendix 2. Chemical Data for the Representative Altered Rocks, Stog'er Tight Prospect

	Measured Composition						Reconstituted Composition††					
Sample(*)	**BN55-B15**	**BN53-13**	**BN53-21**	**BN24-06**	**BN24-09**	**BN24-14**	**BN55-B15**	**BN53-13**	**BN53-21**	**BN24-06**	**BN24-09**	**BN24-14**
Alteration(**)	**Zone I**	**Zone III**	**Zone IV**	**Zone II**	**Zone III**	**Zone IV**	**Zone I**	**Zone III**	**Zone IV**	**Zone II**	**Zone III**	**Zone IV**
Precursor							**BN55-B12**	**BN53-10**	**BN53-10**	**BN24-01**	**BN24-01**	**BN24-01**
SiO_2(f)	45.35	56.60	43.40	39.90	52.35	36.25	34.67	71.08	44.05	39.92	39.14	34.85
TiO_2	2.53	0.66	4.96	1.59	0.71	4.21	1.93	0.83	5.04	1.59	0.53	4.05
Al_2O_3	17.54	12.90	10.30	16.43	21.59	17.03	13.41	16.20	10.45	16.44	16.14	16.37
Fe_2O_3(ff)	13.67	6.68	16.10	9.67	8.02	24.93	10.45	8.39	16.34	9.67	5.99	23.97
MnO	0.18	0.11	0.18	0.13	0.04	0.20	0.14	0.14	0.18	0.13	0.03	0.19
MgO	4.63	1.21	4.39	4.38	1.21	4.72	3.54	1.52	4.46	4.38	0.90	4.54
CaO	9.14	4.94	7.69	9.25	1.36	4.30	6.99	6.20	7.80	9.25	1.02	4.13
Na_2O	3.54	7.60	0.51	1.17	6.37	3.31	2.71	9.54	0.52	1.17	4.76	3.18
K_2O	0.070	0.280	0.780	3.330	2.680	0.700	0.054	0.35	0.79	3.331	2.00	0.67
P_2O_5	0.320	0.660	0.240	0.150	0.320	0.740	0.245	0.83	0.24	0.150	0.24	0.71
Total	96.97	91.65	88.55	86.00	94.65	96.39	74.14	115.09	89.87	86.03	70.76	92.66
S(fff)	46	18673	1871	690	13373	744	35	23450	1899	690	9998	715
Sc	29	10	62	37	10	34	22	13	63	37	8	33
V	310	43	517	272	127	373	237	54	524	272	95	359
Cr	24	ND	ND	86	ND	ND	19	—	—	86	—	—
Ni	14	ND	ND	24	ND	ND	11	—	—	24	—	—
Cu	27	ND	13.0	11	ND	16	21	—	13	11	—	16
Zn	90	ND	113	36	33	196	69	—	115	36	25	188
Ga	15	ND	ND	10	47	28	11	—	—	10	35	27
Rb	2.2	3.5	14.5	47.6	39.0	9.6	1.7	4.4	14.7	47.6	29.2	9.2
Sr	413	205	76	262	107	199	315	258	77	263	80	191
Ba	19	29	76	102	188	51	15	36	77	102	141	49
Y	25.7	31.8	27.4	15.4	73.1	63.1	19.6	39.9	27.9	15.4	54.7	60.7
Zr	179	284	211	123	738	426	137	356	214	123	552	409
Hf	4.14	6.30	5.04	3.78	16.17	10.10	3.16	7.91	5.12	3.78	12.09	9.71
Nb	11.8	17.1	17.1	7.3	37.4	23.6	9.0	21.4	17.4	7.3	28.0	22.7
Th	0.79	1.19	0.67	0.55	3.49	1.85	0.60	1.50	0.68	0.55	2.61	1.78
La	11.64	15.99	10.27	6.64	43.44	25.91	8.90	20.09	10.43	6.64	32.48	24.90
Ce	30.19	41.77	27.66	17.27	108.66	69.85	23.09	52.45	28.07	17.28	81.24	67.14
Pr	4.29	5.85	4.04	2.46	14.69	9.97	3.28	7.35	4.10	2.46	10.98	9.58
Nd	19.55	25.45	19.27	11.26	62.80	46.20	14.95	31.96	19.56	11.27	46.95	44.41
Sm	4.86	6.39	5.07	3.01	15.13	11.88	3.72	8.03	5.14	3.01	11.31	11.42
Eu	1.68	2.28	1.63	1.13	4.74	3.46	1.29	2.86	1.66	1.13	3.54	3.33
Gd	5.09	7.31	5.83	3.10	15.73	12.79	3.89	9.18	5.92	3.10	11.76	12.30
Tb	0.78	1.09	0.94	0.52	2.41	1.94	0.60	1.37	0.95	0.52	1.80	1.87
Dy	4.67	6.68	5.66	3.09	14.80	11.80	3.57	8.39	5.74	3.10	11.06	11.34
Ho	0.97	1.30	1.17	0.64	3.06	2.40	0.74	1.63	1.19	0.65	2.29	2.31
Er	2.62	3.63	3.19	1.81	8.70	6.71	2.01	4.56	3.24	1.81	6.50	6.45
Tm	0.36	0.51	0.42	0.26	1.24	0.92	0.28	0.64	0.43	0.26	0.93	0.89
Yb	2.29	3.09	2.69	1.70	8.14	5.65	1.75	3.88	2.73	1.70	6.08	5.43
Lu	0.35	0.47	0.37	0.27	1.29	0.86	0.27	0.59	0.38	0.27	0.96	0.83

Notes

* Sample numbers starting with BN are from drill-core, the following two digits correspond to drill-hole number (see Fig. 3 for locations).

** Zone I = chlorite-calcite zone, Zone II = ankerite-sericite zone, Zone III = red albite-pyrite zone, Zone IV = chlorite-magnetite zone.

f Major oxide concentrations in percent.

ff Total Fe measured as Fe_2O_3 after complete oxidation of iron by ignition.

fff Trace element concentrations in parts per million.

†† Corrected for net mass gains and losses relative to the unaltered precursors, based on mass balance calculations by the isocon method.

ND = not detected.